Magnetoelectric effect and low-temperature phase transitions of $TbMn_2O_5$

1995 J. Phys.: Condens. Matter 7 2855

(http://iopscience.iop.org/0953-8984/7/14/022)

J. Phys.: Condens. Matter 7 (1995) 2855–2863. Printed in the UK

Magnetoelectric effect and low-temperature phase transitions of $TbMn_2O_5$

Kazuhiro Saito and Kay Kohn
Department of Physics, Waseda University, Shinjuku-ku, Tokyo 169, Japan

Received 24 October 1994, in final form 5 December 1994

Abstract. We made dielectric, magnetic and magnetoelectric measurements on single-crystal samples of $TbMn_2O_5$, which was an antiferromagnet with the Néel temperature of approximately 40 K. From the results, we concluded that there were two groups of phase transitions at lower temperatures. The first group are three successive transitions at 29.3, 27.2 and 25.6 K, whose natures are probably electric. The crystal is polar below this temperature range, because the polarity of the magnetoelectric effect can be controlled by electric field cooling. Another transition exists at 8 K, where time inversion symmetry breaks. It is related to the ordering of Tb^{3+} magnetic moments.

1. Introduction

$TbMn_2O_5$ is one of the oxides in the RMn_2O_5 series, where R is a rare earth from Nd to Lu, Y or Bi [1]. They have a complicated structure where a Mn^{4+} ion is located at the centre of an oxygen octahedron, while a Mn^{3+} ion is at the base centre of a square pyramid. The octahedra share their edges to form a ribbon similar to that in rutile structure. A MnO_5 bipyramid forms a bridge connecting these ribbons. A larger R^{3+} ion is surrounded by eight oxygen atoms [2].

Previous neutron diffraction studies revealed that Mn^{3+} and Mn^{4+} moments were magnetically ordered specified by a propagation vector $q = (\frac{1}{2}, 0, \tau)$ below the Néel temperature T_N around 40 K [3–7]. The value of τ is from 0.24 to 0.37. They reported further magnetic transitions at lower temperatures, where the ordering of the rare-earth moments developed.

Specifically for $TbMn_2O_5$, Buisson [4, 5] proposed a helical magnetic ordering of the Mn spins with $\tau = 0.31$ (at 18 K) and an amplitude-modulated spin-density wave of the Tb^{3+} moments at lower temperatures, based on his powder diffraction data. However, Gardner *et al* [7] made a neutron diffraction study of a single crystal and concluded spin-density waves for both the Mn and the Tb moments. According to their model, the moments are in the a–b plane and in particular the Tb moments are near to the a axis.

Dielectric, magnetic and magnetoelectric studies indicated the possibility that the RMn_2O_5 compounds were ferroelectric in their ordered magnetic phase [8–14]. In particular, it has been suggested that $EuMn_2O_5$ is transformed into a helimagnetic and ferrolectric compound simultaneously at a T_N of approximately 39 K [8–10].

In this context, the magnetoelectric effect is a sensitive tool for detecting the breaking of both space and time inversion symmetries [15]. In particular, in a polar crystal, it has the opposite sign in a domain of opposite polarity.

We selected $TbMn_2O_5$ as a typical example, because Tb^{3+} with the $(4f)^8$ configuration has a large magnetic moment of $9.7\mu_B$ with a large magnetic anisotropy. This oxide is

0953-8984/95/142855+09$19.50

in contrast with $GdMn_2O_5$ which we reported in a previous paper [11]. A Gd^{3+} ion also possesses a large but isotropic magnetic moment of $7.9\mu_B$. We made dielectric, magnetic and magnetoelectric measurements on single-crystal samples of the oxide, which revealed the existence of a series of several phase transitions. There are three successive transitions between 25 and 30 K, below which $TbMn_2O_5$ is a polar crystal. In addition, the crystal loses the time inversion symmetry below the transition at 8 K, where the ordering of the Tb^{3+} magnetic moments probably develops.

2. Experimental methods

2.1. Single crystals

Single crystals of $TbMn_2O_5$ were prepared by the $PbO–PbF_2$ flux method [16]. We prepared two samples for the measurements. Sample A had the dimensions 2.8 mm, 1.4 mm and 3.0 mm along a, b and c axes, respectively. We formed a pair of electrodes of silver paste on b surfaces. The other (sample B) had c surfaces with an area of 3.4 mm^2, on which we formed the electrodes. The thickness was 0.9 mm.

2.2. Measurements of magnetization and dielectric constant

Magnetic measurements were made along the a, b and c directions of sample A with a vibrating-sample magnetometer (PAR-4500). The dielectric constant was determined from the capacitance which was recorded with an impedance analyser (YHP-4192A) with an ordinary AC four-terminal method. The frequency covered was from 1 kHz to 5 MHz. The temperature was detected with an (Au–Fe)–chromel or an (Au–Fe)–normal silver thermocouple in all the measurements including those of the magnetoelectric effect described below. The systematic error between different sets of thermocouples was less than ± 0.5 K.

2.3. Measurements of the magnetoelectric effect

The magnetoelectric effect was measured with an AC $(ME)_H$ method in which the AC magnetoelectric polarization p was induced by an AC magnetic field h of 171 Hz and 25 Oe (RMS). The static bias magnetic field H was applied in some measurements, superposed on the AC field.

The voltage v between the electrodes on the sample is given by

$$v = \frac{pS}{C_0 + C} \tag{1}$$

where S is the area of the electrode, and C_0 and C are the capacitances of the sample and the measuring system, respectively. They were 0.2 pF and 55 pF, respectively. We recorded v with a lock-in amplifier (PAR-124A) tuned with the AC magnetic field. Before each run of measurements, the sample was cooled from 77 to 4.2 K within an electric field of 7 kV cm^{-1} applied along the b or c direction.

Because $TbMn_2O_5$ does not have a large spontaneous magnetization like a ferromagnet, we can regard the effect of applied magnetic fields as a small perturbation on the crystal. In this case the ith component of p is expressed as

$$p_i = \sum \alpha_{i,j} h_j + \sum \beta_{i,kj} H_k h_j + \cdots \tag{2}$$

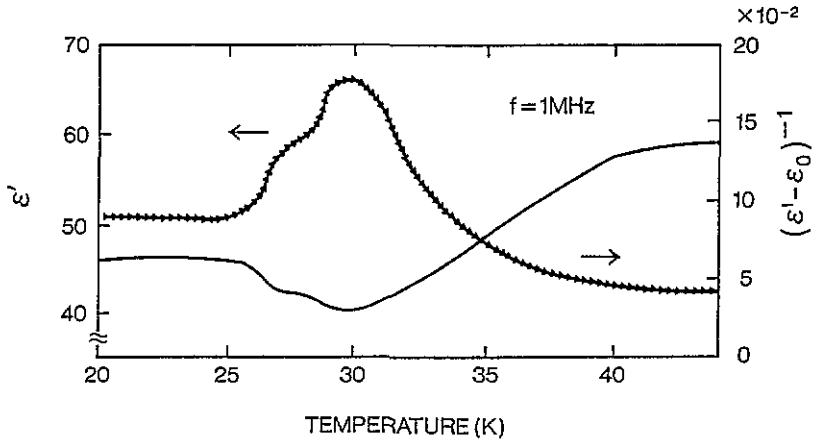

Figure 1. Temperature dependence of dielectric constants along the b axis.

as a function of h_j and H_k, the jth and kth components of the AC and static fields, respectively. The coefficients α_{ij} and $\beta_{i,kj}$ are linear and quadratic (in magnetic field) magnetoelectric susceptibilities, respectively. They take the opposite sign in domains of the opposite polarity in a polar crystal. We can separate linear and quadratic effects by plotting p or the signal voltage v against H. In particular, when H and h are parallel, the signal is proportional to the magnetic field derivative $\partial P/\partial H$ of the magnetoelectric polarization.

3. Results

3.1. Dielectric constant

We depict the temperature dependence of the dielectric constant ϵ_b' along the b direction (sample A) in figure 1. A peak exists at $T_P = 29.3$ K, accompanied by a shoulder at $T_S = 27.2$ K. On the contrary, only a very small peak was observed in the c direction (sample B). The temperatures T_P and T_S were independent of the frequency between 1 kHz and 5 MHz. The dielectric constant ϵ_c' also has a small peak at 29.3 K, but its height is less than 0.5% of that in ϵ_b'. We suppose that this is due to a possibly small misorientation of the sample.

We fitted the recorded data with the Curie–Weiss relation

$$\epsilon' - \epsilon_0 = \frac{C}{T - \Theta}. \tag{3}$$

In the fitting we chose the parameters ϵ_0, C and Θ in such a way that the region of linear dependence between $(\epsilon_b' - \epsilon_0)^{-1}$ and temperature T would be as wide as possible. The result is also shown in figure 1, where the data fall on a straight line in the range 32–40 K. The parameters ϵ_0, C and Θ are equal to 35, 93 K and 28 K, respectively.

3.2. Magnetization

In figure 2 we depict the magnetization curves at 4.2 K in three principal directions. They are linear along the b and c directions. The magnetization at 4.2 K along the a direction

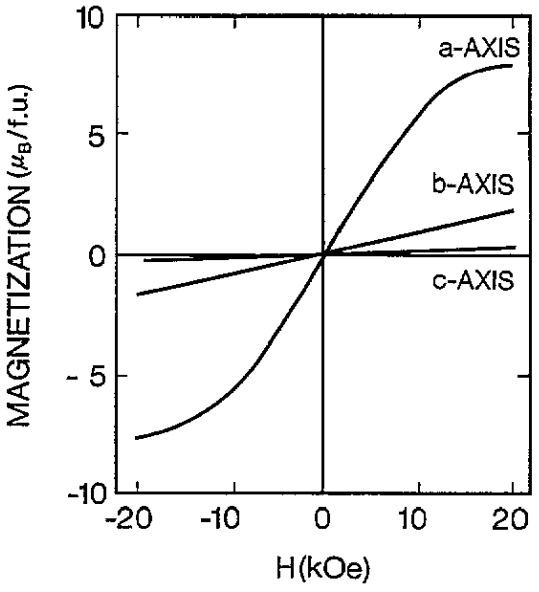

Figure 2. Magnetization curves at 4.2 K along the *a*, *b* and *c* axes.

is much larger and shows a tendency to saturation at higher magnetic fields. The value of magnetization at 18 kOe is $7.7\mu_B$ formula unit, which is comparable with the free-ion value $9.72\mu_B$ for a Tb^{3+} ion. This tendency to saturation is observed up to about 25 K. No other anomaly is observed in magnetization between 4.2 and 273 K.

3.3. Magnetoelectric effect

At 4.2 K, we observed a magnetoelectric signal in several configurations. We summarize the results in tables 1 and 2. The asterisks indicate that we observed a reproducible signal whose sign was reversed after electric field cooling in the opposite direction. The zeros mean that the signal was not observed within the accuracy of our measurements.

Table 1. Magnetoelectric signals observed when the electric field cooling and magnetoelectric polarization were along the *b* axis.

	AC magnetic field		
DC magnetic field	*a*	*b*	*c*
a	*	0	0
b	*	*	*
c	0		*

When a static magnetic field H is applied along the b or c direction, the signal v is almost linear in H as described by the β term in (2). On the other hand, when H is along the a direction, the field dependence of the signal is apparently complicated. For instance, we depict the H-dependence of the magnetoelectric signal at 4.2 K in the $\{\boldsymbol{p} \parallel b, \boldsymbol{h} \parallel a, \boldsymbol{H} \parallel a\}$ configuration in figure 3. However, when we plot $V_{ME} = \int v \, dH$ versus M^2 (figure 4), it is almost linear, showing that the effect is approximately described by the β term in (2).

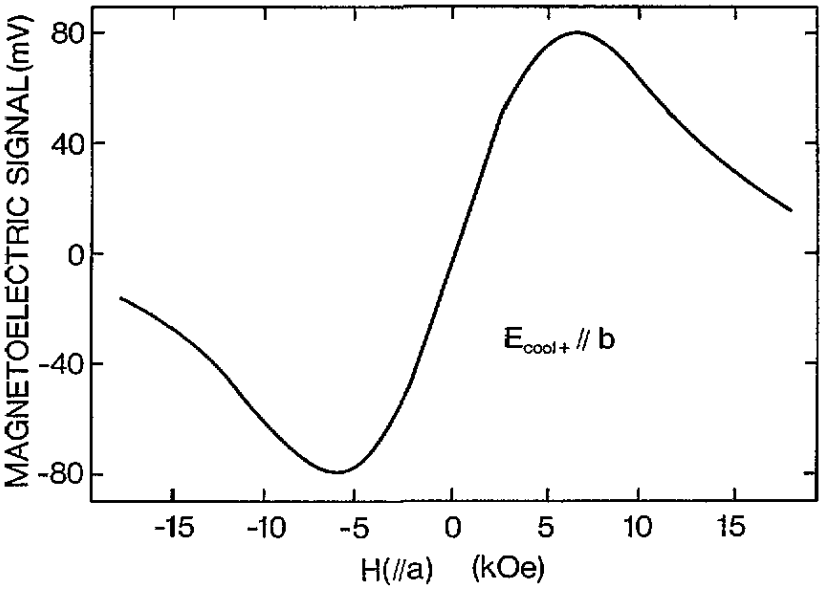

Figure 3. Static field dependence of the magnetoelectric signal in the $\{p \parallel b, h \parallel a, H \parallel a\}$ configuration.

Table 2. Magnoelectric signals observed when the electric field cooling and magnetoelectric polarization were along the c axis.

	AC magnetic field		
DC magnetic field	a	b	c
a	*	*	
b		*	
c			*

In figure 5, we show the overall temperature dependence of the magnetoelectric signal at an intermediate field (5 kOe) in the $\{p \parallel b, h \parallel a, H \parallel a\}$ configuration. It decreases rapidly with increasing temperature from 4.2 K, then indicates a peak at 25.6 K and finally goes to zero at about 40 K. As noted above, this represents approximately the temperature dependence of $\beta_{b,aa}$. Two curves represent the results of the experimental runs after the electric field cooling along the positive (E_{cool+}) and the negative (E_{cool-}) b directions. We note that the signal below about 30 K takes the opposite sign according to the direction of the electric field during cooling. This demonstrates directly that $TbMn_2O_5$ is a polar crystal and its polarization is switched by the applied electric field below this temperature range.

The detail of the temperature dependence around the peak is shown in figure 6(a), where there is a peak at 25.6 K and a shoulder at 27.2 K (T_S). The signals in other configurations also have a structure at T_S. For instance, we show the temperature dependence of the magnetoelectric signal in the $\{p \parallel c, h \parallel a, H \parallel a\}$ configuration in figure 6(b). In this case, we observed two resolved peaks at 25.6 and 27.2 K. The latter coincides with T_S.

Figure 7 shows the temperature dependence of the signal in the $\{p \parallel b, h \parallel a, H \parallel a\}$ configuration under zero (less than 0.1 Oe) static field. Before this run of measurements, the sample was magnetized once at 4.2 K in the magnetic field of 19 kOe along the a direction.

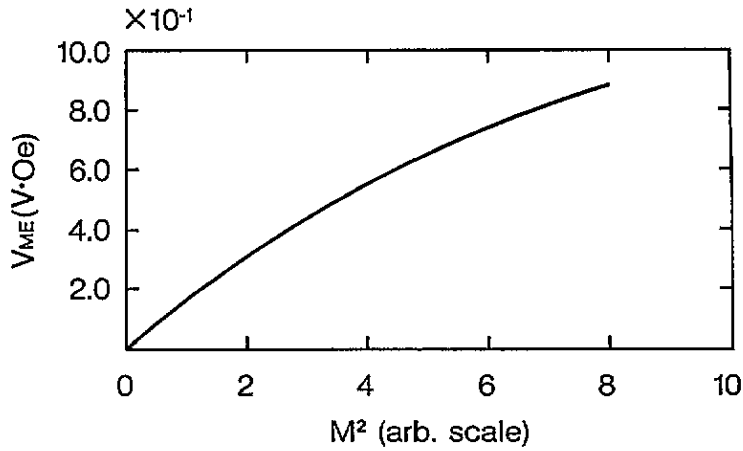

Figure 4. The relation between $V_{ME} = \int v\,dH$ and M^2 in the $\{p \parallel b, h \parallel a, H \parallel a\}$ configuration.

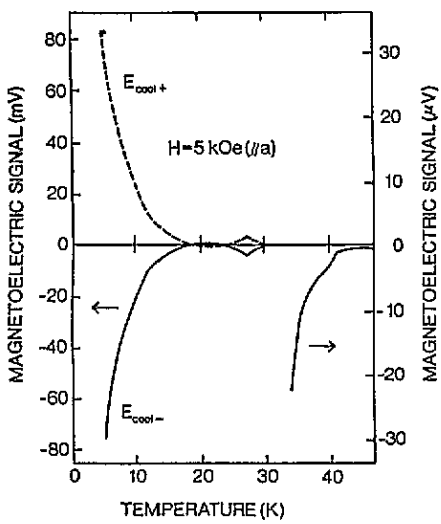

Figure 5. Temperature dependence of the magnetoelectric signal (at the bias field of 5 kOe) in the $\{p \parallel b, h \parallel a, H \parallel a\}$ configuration. Two curves correspond to opposite directions of the electric field applied during cooling the sample to 4.2 K.

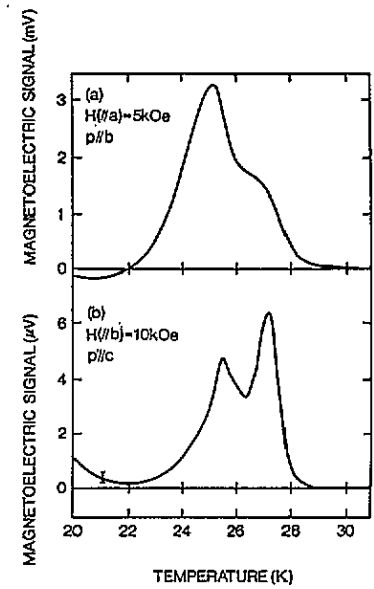

Figure 6. Temperature dependence between 20 and 30 K of (a) the magnetoelectric signal (at the bias field of 5 kOe) in the $\{p \parallel b, h \parallel a, H \parallel a\}$ configuration and (b) the magnetoelectric signal (at the bias field of 10 kOe) in the $\{p \parallel c, h \parallel a, H \parallel a\}$ configuration.

The signal possessed an opposite sign in the state of the opposite remanent magnetization.

For comparison, we also display the temperature dependence of the signal at the static field of 5 kOe. At 4.2 K, the signal at zero bias field has the opposite sign to the signal at 5 kOe and decreases rapidly with increasing temperature. Its magnitude at 8 K is about one tenth of that at 4.2 K. This is described by the quadratic effect, as we noted above.

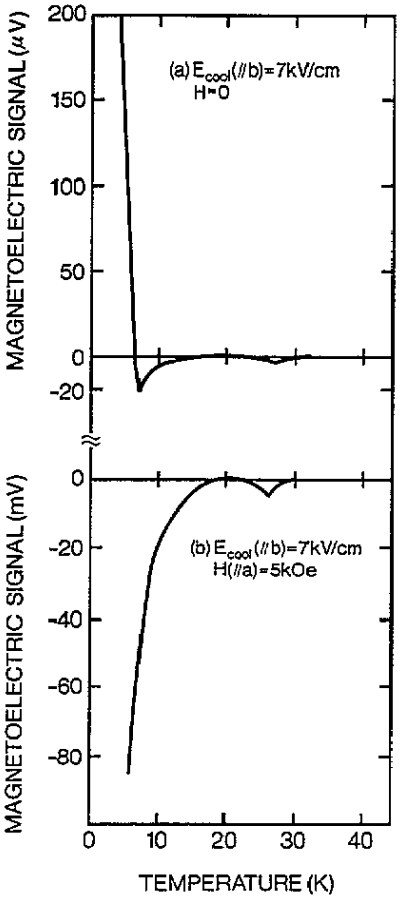

Figure 7. Temperature dependence of the magnetoelectric signal in the $\{p \parallel b, h \parallel a, H \parallel a\}$ configuration: (a) zero bias field; (b) 5 kOe bias field.

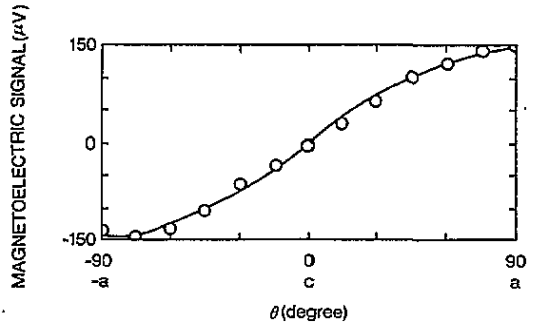

Figure 8. Dependence of the magnetoelectric signal on the direction of the AC magnetic field within the a–c plane (at zero bias field).

We depict the dependence of the zero-field signal on the direction of the AC magnetic field in the a–c plane in figure 8. It is typical for a property described by a second-rank

tensor.

These facts indicate that the linear magnetoelectric effect exists below approximately 8 K, which gives rise to the zero-field signal. From figure 8, we conclude that α_{ba} is 1.6×10^{-5} (in cgs G units) at 4.2 K, while α_{bc} is zero.

4. Discussion

4.1. Phase transitions at 29.3, 27.2 and 25.6 K

The anomalies in the temperature dependence of both the dielectric and the magnetoelectric susceptibilities indicate the existence of successive electric transitions at 29.3, 27.2 and 25.6 K. Similar transitions have been reported for other oxides of the RMn_2O_5 series [8–14].

The dependence of the polarity of the magnetoelectric effect on the sense of the electric field during cooling shows that the crystal is polar below 29.3 K. This suggests the possibility of ferroelectric ordering in $TbMn_2O_5$ below this transition temperature, although the peak value of the dielectric constant is smaller than that in typical ferroelectric crystals. In preliminary trials to detect pyroelectricity, we observed a sharp rise in pyroelectric current at 28 K [17].

4.2. Phase transition at 8 K

The appearance of a linear magnetoelectric effect indicates that $TbMn_2O_5$ loses the time inversion symmetry below 8 K. This transition is supposed to be related to the ordering of Tb^{3+} moments.

Previous neutron diffraction studies revealed the ordering of the magnetic moments of rare-earth ions at low temperatures. For instance, the Dy^{3+} moments order below 8.4 K in $DyMn_2O_5$ [6]. This transition was specified with the rapid increase in the intensity of some magnetic reflections with decreasing temperature. A similar temperature dependence was also reported for $ErMn_2O_5$ [7]. These results seem to support a view that the ordering of Tb^{3+} moments develops in the temperature range around 10 K.

Gardner *et al* [7] proposed that the magnetic structure of $TbMn_2O_5$ was amplitude-modulated spin-density waves, where the Tb^{3+} moments had a large component along the a axis [7]. This structure is consistent with our result that the susceptibility along the a direction was much larger in comparison with other directions. However, the linear magnetoelectric effect is not allowed in the supposed magnetic symmetry $P_{2a}m'c'2_1$.

4.3. Magnitude of magnetoelectric susceptibilities

The observed magnetoelectric effect is very large below about 10 K. For instance, the value of $\beta_{b,aa}$ at 4.2 K is 2×10^{-6} (in cgs G units). It is about 30 times that in $GdMn_2O_5$, which is 6×10^{-8}. It is a natural result, when we consider that the magnetoelectric effect below 8 K is mainly determined by an anisotropic Tb^{3+} ion with larger spin–lattice coupling than a spherical Gd^{3+} ion. This difference was reported with respect to the linear magnetoelectric effect in $Tb^{3+}AlO_3$ [18] and $Gd^{3+}AlO_3$ [19].

The value of α_{ba} is about one tenth of the maximum value of Cr_2O_3, which is a typical substance with a linear magnetoelectric effect.

5. Summary

In conclusion, $TbMn_2O_5$ shows three successive transitions at 29.3, 27.2 and 25.6 K. They are characterized by the anomalies in dielectric constant and/or magnetoelectric susceptibility and are probably of an electric nature. The crystal is polar below these transitions as shown by the dependence of the magnetoelectric effect on the electric field applied during cooling of the crystal to 4.2 K.

Another transition exists at 8 K. The magnetoelectric effect linear in the magnetic field appears below this temperature, which indicates the breaking of time inversion symmetry in the low-temperature phase. This transition is considered to be related to the ordering of Tb^{3+} magnetic moments. The magnitude of second-order magnetoelectric susceptibility is very large especially below this transition.

Acknowledgments

The authors offer their sincere thanks to Akinobu Ikeda, Akihiro Inomata and Seiichi Kato for their assistance in the experiments. This work was partly supported by a Grant-in-Aid for Scientific Research from the Ministry of Education, Science and Culture and a Murata Science Foundation Grant.

References

[1] Quézel-Ambrunaz S, Bertaut E F and Buisson G 1964 *C. R. Acad. Sci., Paris* **258** 3025
[2] Abrahams S C and Bernstein J L 1967 *J. Chem. Phys.* **46** 3776
[3] Bertaut E F, Buisson G, Quézel-Ambrunaz S and Quézel G 1967 *Solid State Commun.* **5** 25
[4] Buisson G 1973 *Phys. Status Solidi* a **16** 533
[5] Buisson G 1973 *Phys. Status Solidi* a **17** 191
[6] Wilkinson C, Sinclair F, Gardner P, Forsyth J B and Wanklyn B M R 1988 *J. Phys. C: Solid State Phys.* **14** 1671
[7] Gardner P, Wilkinson C, Forsyth J B and Wanklyn B M R 1988 *J. Phys. C: Solid State Phys.* **21** 5653
[8] Sanina V A, Sapozhnikova L M, Golovenchits E I and Morozov N V 1988 *Sov. Phys.–Solid State* **30** 1736
[9] Golovenchits E I, Morozov N V, Sanina V A and Sapozhnikova L M 1992 *Sov. Phys.–Solid State* **34** 56
[10] Doi T and Kohn K 1992 *Phase Transitions* **38** 273
[11] Tsujino H and Kohn K 1992 *Solid State Commun.* **83** 639
[12] Tsujino H, Komada H, Tanaka Y and Kohn K 1992 *Proc. 6th Int. Conf. on Ferrites (Tokyo and Kyoto, 1992)* ed M Abe and T Yamaguchi (Tokyo: Japan Society of Powder and Powder Metallurgy) p 714
[13] Kohn K 1994 *Ferroelectrics* at press
[14] Tanaka Y, Saito K, Tsujino H and Kohn K 1995 *Ferroelectrics* at press
[15] Siratori K, Kohn K and Kita E 1992 *Acta Phys. Pol.* A **81** 431
[16] Wanklyn B M R 1972 *J. Mater. Sci.* **7** 813
[17] Inomata A, Saito K and Kohn K 1994 unpublished
[18] Mercier M and Cursoux M 1968 *Solid State Commun.* **6** 207
[19] Mercier M and Velleaud G 1971 *J. Physique Coll.* **32** C1 499